Characterizing dynamic functional connectivity in congenitally blind people using Hidden Markov Models

Authors: Caterina A. Pedersini [1,2], Bas Rokers [1-3], Olivier Collignon [4,5]

1. Division of Science, New York University, Abu Dhabi, NYUAD
2. ASPIRE Precision Medicine Research Institute, Abu Dhabi, UAE
3. Center for Brain and Health, New York University, Abu Dhabi, NYUAD
4. Institute of Psychology (IPSY) & Institute of Neuroscience (IoNS), UCLouvain, Louvain-la-Neuve 1348, Belgium
5. HES-SO Valais-Wallis, The Sense Innovation and Research Center, Lausanne 1007 & Sion 1950, Switzerland

Corresponding author:
Caterina Annalaura Pedersini
cpedersini86@gmail.com

Acknowledgements: This research is supported by the NYUAD Center for Brain and Health, funded by Tamkeen under NYU Abu Dhabi Research Institute grant CG012. The ASPIRE Precision Medicine Research Institute Abu Dhabi (ASPIREPMRIAD) awarded grant number VRI-20-10 by ASPIRE, the technology program management pillar of Abu Dhabi's Advanced Technology Research Council (ATRC). We wish to extend our gratitude to Marco Barilari for sharing the data and providing details about the acquisition protocols. We are also extremely thankful to our blind participants for their invaluable contributions.

Abstract

How does sensory experience influence the brain connectome? Early acquired blindness is known to trigger a large-scale alteration in brain connectivity. Previous studies have traditionally assessed stationary functional connectivity across all timepoints in scanning sessions. In this study we compared the dynamic nature of functional connectivity in sighted (50) and early/congenitally blind (33) individuals through the data-driven approach of Hidden Markov Models (HMM).

Blind individuals showed increased fractional occupancy in two key brain states: one characterized by bilateral somatomotor activation and another by occipito-frontal activation, mainly in the left hemisphere. Conversely, sighted individuals more frequently occupied a state associated with Default Mode and Ventral Attentional networks. Network analysis revealed decreased connectivity in blind individuals within states frequently occupied by sighted individuals, particularly between visual and somatomotor regions. In contrast, states more often visited by blind individuals exhibited increased connectivity within the visual network, connecting multiple occipital regions with the temporal fusiform area, as well as between visual and prefrontal regions. These results suggest that the frequency of visiting specific brain states may contribute to the differences observed between blind and sighted individuals in stationary resting state functional connectivity.

Together, these findings show the effectiveness of Hidden Markov Models in capturing the temporal dynamics of functional connectivity, revealing its variability over time. We found that early visual deprivation disrupts these dynamics, with blindness leading to prolonged activation of unimodal regions and increased connectivity within the visual network and between occipital and higher-order brain regions. Additionally, alterations in the chronnectome, defined as the functional connectome changing over time - specifically in the time spent visiting a state - may provide new insights into stationary functional connectivity patterns in blind individuals, establishing a foundation for understanding network connectivity dynamics following sensory deprivation.

Introduction

The study of individuals who experience visual deprivation early in life provides a unique model to explore how the brain's structural and functional architecture adapts following sensory deprivation. In early blind individuals, functional brain plasticity has been observed through either alteration of activity in non-deprived sensory regions, defined as intramodal plasticity (Elbert et al., 2002; Hertrich et al., 2013) or enhanced processing of non-visual sensory information in deprived sensory area, defined as crossmodal plasticity (Frasnelli et al., 2011; Neville & Bavelier, 2002 for a review). Whereas the recruitment of occipital regions by nonvisual inputs in the congenitally blind highlights its dependence upon experience to organize itself, the observation of specialized cognitive modules in the occipital cortex of congenitally blind, similar to those observed in the sighted, highlights the intrinsic constraints imposed to such plasticity (Collignon et al., 2011; Dormal & Collignon, 2011; Makin & Krakauer, 2023; Mattioni et al., 2020; Reich et al., 2012; Ricciardi et al., 2014).

To better understand how the occipital regions in early blind individuals (EBs) are organized to support sensorimotor and cognitive functions, it is essential not only to examine their response properties (functional specialization) but also to explore how these regions are integrated into broader brain networks (functional integration) (Friston et al., 2003). A widely used approach for studying both short- and long-range functional brain interactions is functional connectivity (FC). FC quantifies the temporal correlation of functional activity between different brain regions, often expressed as pairwise Pearson's correlation coefficients between time series (Smitha et al., 2017). Traditional research on functional connectivity following early visual deprivation has primarily focused on group-level patterns, consistently revealing increased or decreased connectivity involving occipital regions (see Bock & Fine, 2014 for a review). Among the most reliable findings is a reduction in functional connectivity between occipital and non-visual (eg tactile or auditory) sensory cortical areas (Abboud & Cohen, 2019; Bauer et al., 2017; Burton et al., 2014; Liu et al., 2007; Pelland et al., 2017; Striem-Amit et al., 2015; Wen et al., 2018).

This well-established finding appears counterintuitive when compared to numerous studies that report enhanced task-dependent activation in occipital regions during the processing of auditory and tactile inputs in EBs (see Bavelier & Neville, 2002; Frasnelli et al., 2011 for review). Notably, the functional significance of occipital activity in the non-visual sensory and perceptual processing of early blind individuals is reinforced by studies demonstrating impaired performance in specific tactile and auditory tasks following the disruption of the occipital cortex via transcranial magnetic stimulation (TMS) (Cohen et al., 1997; Collignon, Davare, et al., 2009; Collignon et al., 2006). Additional evidence comes from studies investigating effective (causal) connectivity (Friston, 1994), using dynamic causal modeling of fMRI data (Friston et al., 2003) or the combination of TMS with Positron Emission

Tomography (PET), which measures activity in distant cortical regions stimulated by TMS. These studies have shown stronger coupling between auditory or somatosensory areas and occipital regions in EBs (fMRI: Collignon et al., 2013; Klinge et al., 2010; PET and TMS: Wittenberg et al., 2004). Finally, the involvement of the occipital cortex in non-visual processes in response to stimulus presentation (Collignon, Voss, et al., 2009; Leclerc et al., 2000; Müller et al., 2019; Röder et al., 1999) suggests the existence of direct connections between the occipital cortex and other non-visual sensory regions. These findings align with evidence from fiber tracing studies in primates (Falchier et al., 2002; Rockland & Ojima, 2003) and tractography in humans (Beer et al., 2011), which demonstrate the presence of direct connections between auditory and visual cortices.

Traditional FC analysis assumes that interactions between brain regions remain stable over time. However, a novel approach suggests that the wandering mind transitions between multiple functional modes, resulting in dynamic functional connectivity (dFC), meaning patterns of FC changing over time despite the absence of a cognitive task. Consequently, connectivity measured over an entire run may reflect an average of these states, with weak or strong connectivity patterns influenced by the predominance of a specific state. These fluctuations in connectivity could represent the functional capacity of neural systems (Deco et al., 2011; Kucyi et al., 2017) and may serve as a promising biomarker for disease (Damaraju et al., 2014; Hutchison et al., 2013).

The most common way to assess dFC is represented by the use of *fixed sliding time windows*, in which the entire fMRI data are segmented in sub-portions of time series (Menon & Krishnamurthy, 2019) and stationary functional connections between different brain areas are assessed within each one of them (Savva et al., 2019). Recently, this approach has been used to assess abnormal brain functions in clinical populations (Carbo et al., 2017; Kim et al., 2017; Pelland et al., 2017; Watanabe & Rees, 2017). In particular, this method has been used to show higher temporal variability of occipito-temporal resting state FC in EBs, suggesting that occipital regions in this population may play the role of a multiple-demand system (Pelland et al., 2017).

However, this approach comes with some a-priori decisions that can widely affect the results, such as the length and the number of fixed time windows used (Hutchison et al., 2013). The data-driven approach relying on *Hidden Markov Models* (HMM) has recently been developed to overcome these limitations and to study the temporal fluctuations of the brain's large-scale network dynamics (Cao et al., 2019; Kottaram et al., 2019; Moretto et al., 2022, 2023; Quinn et al., 2018; Taghia et al., 2018; Van Schependom et al., 2019; Vidaurre et al., 2016). HMM are models used to identify hidden brain states that represent unique and global brain networks of distinct activity and functional connectivity that repeat at different points in time. The HMM provides information regarding how active each brain state is in time, without using any fixed time window, and how likely is the probability of transitioning from one state to another. Multiple metrics that are extracted from the HMM at subject level, such as the

switching rate (SR) and the proportion of time spent visiting each state (fractional occupancy, FO), are used to describe the *chronnectome*, that defines the functional connectome changing over time. This method, for instance, revealed the presence of a temporal hierarchy in which brain states are organized in two consistent and reproducible metastates: a metastate that covers high cognitive functions and a metastate that covers sensorimotor systems and perception. The proportion of time spent visiting a specific brain state or metastate represents a subject-specific and heritable feature that can predict individual behavioral traits (Vidaurre et al., 2017).

In this study, we assessed dFC in resting-state fMRI data from early blind and sighted individuals to address two main objectives. First, we aimed to examine whether early visual deprivation leads to alterations in the temporal dynamics of functional connectivity. Since visual deprivation before the closure of the sensitive period of visual development (Röder et al., 2021) is known to induce widespread brain changes, we hypothesize that it will result in distinct temporal dynamics, particularly involving unimodal regions. Second, we sought to determine if these dynamic changes offer insights into the differences observed in stationary functional connectomes. Specifically, we aimed to assess whether altered connectivity dynamics can provide insights on the unexpected reduction in connectivity between occipital and sensorimotor regions. To investigate these questions, we applied Hidden Markov Models (HMM) to resting-state fMRI data from both blind and sighted individuals, examined between-group differences in *chronnectome* patterns, and linked these findings to large-scale topographical differences in the functional connectome.

Material and method

Participants

In this study we integrated two datasets collected at different times and locations to bolster statistical power. Each dataset comprised EBs and age- and gender-matched sighted controls. The first dataset was obtained in Trento, Italy, in 2023, consisting of forty-eight native Italian speakers, 16 early blind (10 female, mean age=32.8, std=4.6) and 32 sighted (17 female, mean age=30.4, std=7.5). Further details are available in (Xu et al., 2023). The second dataset, gathered in Montreal, Canada, in 2017, comprised thirty-five subjects, 17 congenitally blind (7 female, mean age=51, std=14.33) and 18 sighted (7 female, mean age = 52.11, std = 12.42). None of the participants had a history of neurobiological or psychiatric disorders.

Data acquisition

The two datasets were acquired using the following protocols:

Dataset 1 (2023). MRI data were collected at the Center for Mind/Brain Sciences, University of Trento (Italy), using a MAGNETOM Prisma 3T MR scanner (Siemens) equipped with a 64-channel head-neck

coil. Functional imaging utilized a simultaneous multislice echoplanar imaging sequence, with a scanning plane parallel to the bicommissural plane and a phase encoding direction from anterior to posterior. Parameters included a repetition time (TR) of 1000 ms, echo time (TE) of 28 ms, and a flip angle (FA) of 59°, with a multiband factor of 5. For both the early blind and sighted control groups, as well as seven participants in the independent sighted group, images were acquired at a spatial resolution of 3 mm, with a field of view (FOV) of 198 mm × 198 mm, a matrix size of 66 × 66, and 65 axial slices. Slice thickness (ST) was set to 3 mm, with a 0.3 mm gap, resulting in voxel dimensions of 3 × 3 × (3 + 0.3) mm. For the remaining nine participants in the independent sighted group, a higher spatial resolution of 2 mm was employed, with a FOV of 200 mm × 200 mm, a matrix size of 100 × 100, and 65 axial slices. Here, slice thickness was reduced to 2 mm, with a 0.2 mm gap, resulting in voxel dimensions of 2 × 2 × (2 + 0.2) mm. Three-dimensional T1-weighted images were acquired using a magnetization-prepared rapid gradient-echo sequence in the sagittal plane, with parameters including a TR of 2,140 ms, TE of 2.9 ms, inversion time of 950 ms, FA of 12°, FOV of 288 mm × 288 mm, a matrix size of 288 × 288, and 208 continuous sagittal slices. Slice thickness was 1 mm, resulting in voxel dimensions of 1 × 1 × 1 mm.

Dataset 2 (2017). MRI data were collected in Montreal (Canada), using a Siemens Prisma fit 3T MR scanner equipped with a 32-channel head-neck coil. Functional imaging utilized a simultaneous multislice echoplanar imaging sequence, with a scanning plane parallel to the bicommissural plane and a phase encoding direction from anterior to posterior. Parameters included a repetition time (TR) of 785 ms, echo time (TE) of 3 ms, and a flip angle (FA) of 54°, with a multiband factor of 3. For both the early blind and sighted control groups images were acquired at a spatial resolution of 3 mm, with a field of view (FOV) of 192 mm × 192 mm, a matrix size of 64 × 64, and 42 axial slices. Slice thickness (ST) was set to 3 mm, resulting in voxel dimensions of 3 × 3 × 3 mm. Three-dimensional T1-weighted images were acquired using a magnetization-prepared rapid gradient-echo sequence in the sagittal plane, with parameters including a TR of 2,300 ms, TE of 2.26 ms, inversion time of 900 ms, FA of 8°, FOV of 288 mm × 288 mm, a matrix size of 256 × 256, and 176 continuous sagittal slices. Slice thickness was 1 mm, resulting in voxel dimensions of 1 × 1 × 1 mm.

MRI data preprocessing

The MRI scans were organized into the Brain Imaging Data Structure (BIDS) format using *dcm2bids* (Gorgolewski et al., 2017) and *dcm2niix* (Li et al., 2016). Subsequently, the images underwent preprocessing using the fMRIPrep pipeline (Esteban et al., 2019) version 20.2.3. This pipeline included motion correction (*mcflirt*), spatial normalization, co-registration between functional and anatomical scans (*bbregister*), and resampling into standard space (MNI, 3mm). Following preprocessing, we performed ICA-based denoising (Griffanti et al., 2014) at the subject level by manually classifying motion and signal components. Approximately 8% of the components were retained (with 92%

classified as noise) in both groups and datasets. The clean data were then temporally filtered using a bandpass filter with frequencies ranging from 0.01 to 0.1 Hz to remove noise, enhance the signal-to-noise ratio, and focus on the slow fluctuations of interest.

To account for potential differences between blind and sighted individuals, we utilized an Atlas parcellation approach instead of conducting a group spatial-ICA. Specifically, we employed the Schaefer Atlas (Schaefer et al., 2018), which consists of 100 parcels corresponding to seven resting-state networks (Yeo et al., 2011): visual, somatomotor, dorsal and salience attention, limbic, frontoparietal, and default mode network. Subsequently, the functional data were coregistered to the Atlas space (MNI, 2mm), and the first eigenvariate was extracted from each parcel using *fslmeants* (*-eig*). This procedure calculates the principal component(s) of the time series within each parcel, providing a single time series that summarizes the dominant pattern of activity while accounting for the highest variance in the parcel's time series. To ensure consistency in the number of volumes across datasets, the first 16 volumes from dataset1 and the first 8 volumes were removed from dataset2, resulting in 464 volumes for each subject. These timecourses will serve as the input for the subsequent Hidden Markov Model (HMM) analysis.

Hidden Markov Model

In this study, we adopted a methodology previously outlined in (Vidaurre et al., 2017), to estimate the temporal dynamic of hidden states by leveraging the HMM-MAR toolbox (Vidaurre et al., 2016) which is available in MATLAB via the public repository (https://github.com/OHBA-analysis/HMM-MAR). We utilized the first eigenvariate extracted from each parcel of the Schaefer Atlas (Schaefer et al., 2018) for each subject, as input data. Prior to inferring the hidden states, we standardized the subject-specific timecourse of each parcel to have a zero mean and unit standard deviation. Subsequently, we temporally concatenated these standardized values to create a data matrix with dimensions N x V, where N=100 (number of parcels), and V=38512 (total number of volumes: 83 subjects * 464 volumes). The HMM was then applied to the concatenated data to derive a unified set of brain states shared among all subjects. Despite this commonality in states, the time series depicting the probability of each brain state activation over time and the proportion of time allocated to each state were estimated at the subject level. Finally, we executed a subject-specific HMM using a dual-estimation process to acquire a comprehensive subject-specific description of time-varying functional connectivity and transition probability matrices. These individualized estimates empower us to conduct between-group statistical analyses on the patterns of transition probability and functional connectivity when a state K was active.

Inference

The HMM serves a probabilistic framework that applies variational Bayes inference to extract an approximation of the model posterior distribution of hidden states (K) inputting the observable data,

that is each parcel's timecourse. Each of these hidden states has a certain probability distribution over time and represents a distinct spatiotemporal pattern of activation.

In this study we used a multivariate Gaussian observation model, that states a Gaussian distribution of the fMRI data, wherein each state is represented by a specific mean activity and covariance matrix. Given the high number of parcels included (100, atlas based) and the reduced number of timepoints (464 volumes), we opted to estimate the hidden states using a Gaussian observational model within a low-dimensional space (PCA space), retaining 10 components (Vidaurre, 2021). When we attempted to infer the hidden states without any dimensionality reduction, we encountered a lack of discernible single-subject temporal dynamics. This implies that each subject was merely described by a single state persisting over time. The parameters fitted to the HMM on reduced data (PCA) encompass: 1) a vector of the state-specific mean activity for each parcel, when the state *K* is active (options.zeromean = 0) ; 2) the variance-covariance matrices of N x N, where N represents the number of parcels (100), when each state is active (options.covtype = 'full'); 3) the probabilities of transitioning from one state to another, at any time point. For initialization, we employed a mixture of Gaussian models with 10 optimization cycles and 3 repetitions. From these repetitions, the one exhibiting the most favorable Free Energy (FE) was selected as the starting point for the inference run. Recognizing the nonlinearity inherent in the Variational Bayes algorithm, we repeated the estimation process 20 times. Subsequently, we ranked these repetitions based on FE, ultimately selecting the one with the lowest value.

Choice of the model size

The selection of the total number of hidden states is a critical parameter that requires a priori specification before initiating the inference process. Prior studies have explored a range of hidden states from 5 to 12 in humans (Baker et al., 2014; Damaraju et al., 2014; Kottaram et al., 2019; Moretto et al., 2022, 2023; Vidaurre et al., 2017). In our investigation, we trained the model with a broader range of states, spanning from 2 to 15.

From each model, we extracted metrics such as Free Energy and Average Log-Likelihood (avLL). However, the Free Energy displayed a tendency to decrease with the increase in the number of states without exhibiting any local minima, rendering it unreliable as a criterion for selecting the model's number of states (see Fig. S1). Similarly, the avLL consistently assumed negative values with a monotonic trend, making it challenging to discern a maximum peak. Although we computed the Akaike Information Criterion (AIC) and Bayesian Information Criterion (BIC), they invariably favored the lowest order (*K*=2) as the optimal choice, potentially influenced by the negative avLL values. Given these limitations, we sought alternative measures to inform our decision-making process. First of all, we visually inspected the within-subject dynamics of hidden states to assess whether, in the specific model order, we could extract the single-subject temporal dynamic of hidden states. To do that, for each subject we plotted multiple measures estimated by the HMM: 1). Gamma, that is the time series of

probability of state activation as a function of time; 2). the Viterbi path, that is the vector showing the most probable a posteriori state and 3). the Transition Probability Matrix, that is the matrix with the probability of transitioning from one specific state to another (see Fig. 1, panel A for data of a representative subject). We observed that, within the 5-9 state range, all subjects exhibited temporal dynamics of functional connectivity. However, beyond this point, we noticed a reduced temporal dynamics mainly in two sighted individuals, belonging to the Dataset2, forcing them to be excluded from the analysis (see Fig. S2). Thus, we chose the range 5-9 as the suitable range for model order. Then, we extracted the ratio of coefficient of variation (CV) of the estimates for each model (Moretto et al., 2022, 2023), to quantify the reliability of the mean estimates as the model order increases. Finally, we explored the distribution of mean activations and distances between pairs of functional connectivity matrices, by means of geodesic distance and pearson dissimilarity (Venkatesh et al., 2020), hypothesizing that lower correlations and greater distances would indicate more independent states. Our comprehensive analysis pointed to 7 as a strong candidate for the chosen model order. Indeed, within the chosen range, Model 7 displayed the lowest CV ratios (with a ratio of CV=0.12), as well as the most favorable combination of low correlation between mean activations and high distance between FC matrices. Thus, we decided to proceed with 7 as the chosen model order. Nonetheless, we conducted analyses for all orders within the 5-9 range and compared mean activation maps to ensure consistency across model orders.

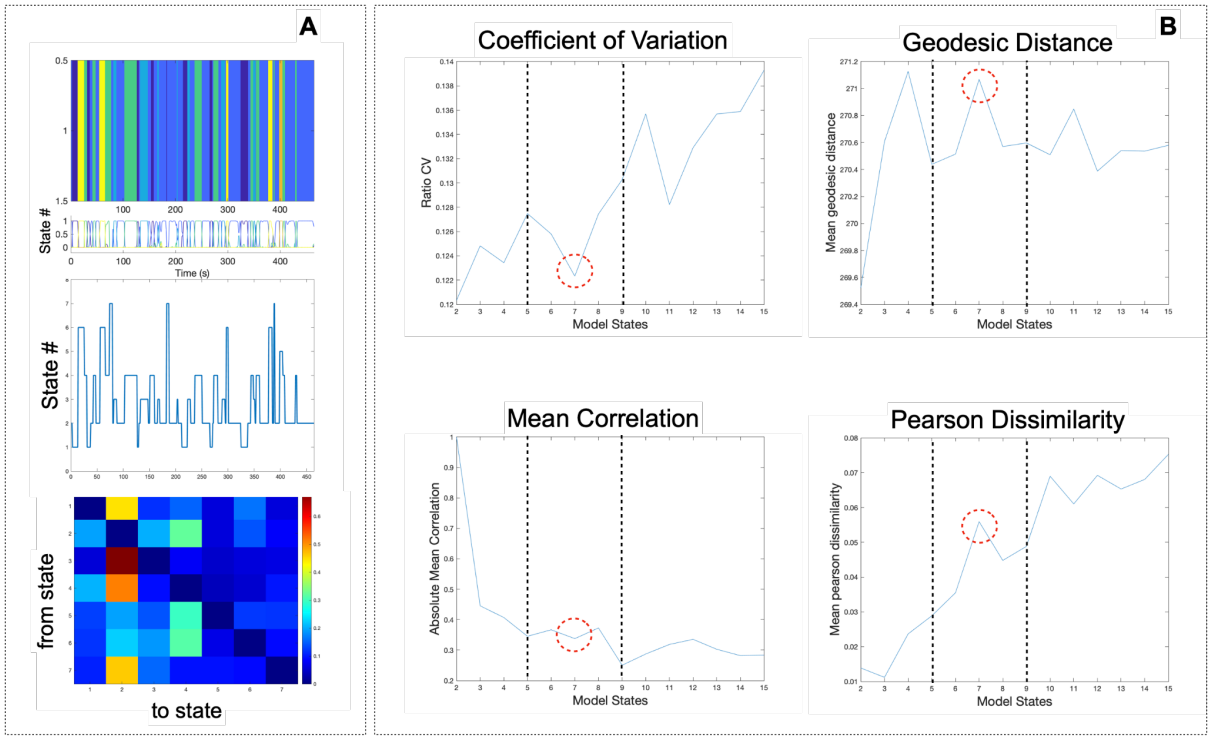

Figure 1. Choice of the model size. Visualization of the criteria used to select the order of the HMM. A: Visualization of Gamma (upper), Viterbi Path (middle) and transition probability (bottom) for one subject from Dataset 2. B. Multiple measures extracted from each model order: Coefficient of Variation, as a measure of reliability of mean estimates as the model order increases; Mean Correlation, Geodesic Distance and Pearson Dissimilarity as measures of independence of hidden states.

Lower correlation and higher distance between functional connectivity matrices highlight the presence of more independent states. The dashed red circle indicates the chosen model order.

Chronnectome

The primary aim of this study is to investigate disparities in the temporal dynamics of functional connectivity between early blind and sighted individuals. To achieve this, we conducted analyses on three key metrics defining the "Chronnectome", employing a GLM-based permutation testing approach (*hmmtest* function within HMM-MAR toolbox) adjusted to include the mean lifetime, without including the transition probability matrices in the analysis. Our design matrix incorporated the fixed-effect of interest, namely, the grouping variable, and three covariates of no interest: mean framewise displacement to account for motion artifacts (a single value per subject), scanner type and age. To address multiple comparisons, we applied False Discovery Rate (FDR) correction with an alpha level set at 0.025. Between-group differences were evaluated based on *Gamma,* which estimates the probability of each state to be active over time, at subject level. This probability is used to extract the three metrics under comparison: (1) fractional occupancy, representing the average state probability across time for each subject and yielding an N x K matrix, where N is the number of subjects (83) and K is the number of states (7); (2) mean lifetime or dwell time, indicating the number of time points spent per visit to a given state; and (3) switching time, representing the mean frequency of switching between one state and another and serves as a measure of stability (one value per subject). These analyses collectively offer insights into the dynamic temporal patterns characterizing the neural dynamics of early blind and sighted individuals.

Functional connectivity

The second aim of this study is to determine whether the alterations in temporal dynamics offer insights into differences observed in stationary functional connectomes. For this reason, we investigated large-scale topographical disparities in the functional connectome derived from blind and sighted individuals, by employing the Network-Based Statistic Toolbox (NBS) in MATLAB, as outlined by (Zalesky et al., 2010). NBS represents a nonparametric statistical approach that extends the cluster-based method used in mass univariate hypothesis testing from physical to topological space, where a cluster's equivalent is a graph component. This allows for the identification of interconnected regions exhibiting significant between-group differences in functional connectivity, providing insights into the network-level between-group differences.

Utilizing subject-specific HMM, we derived functional connectivity matrices at individual level, resulting in N x N matrices where N represents the number of parcels (100) when each state K is active. This yielded seven functional connectivity matrices per subject. In addition, we extracted the time-averaged functional connectome for each subject, that is the functional connectivity that remains stable

over time. To reconstruct the time-averaged functional connectivity we extracted a weighted average of the covariance matrices of states (representing FC) for each subject (100 by 100), where the weights are determined by the fractional occupancies, which represent the total proportion of time spent in each state by each subject (Vidaurre et al., 2021). To facilitate group-level comparisons, these single-subject matrices underwent Fisher's r-to-z transformation. The design matrix used in the NBS analysis integrates the fixed effect of the group alongside mean framewise displacement, scanner type and age as covariates of no interest, mirroring our previous design matrix. We set the primary statistic threshold to 4 to identify supra-threshold connections, and we executed 10,000 permutations to ensure robust statistical inference. Controlling for family-wise error rate at 5%, we scrutinized the resultant network to elucidate significant between-group differences in the total number of connections (*extent*) across the brain's parcellated regions.

Results

States characterization

To delineate the spatial layout of each hidden state, we derived a mean activation vector for each state. These vectors, spanning across 100 parcels, encapsulate the activation levels of each parcel when a specific state (K) is active. In Fig. 2, we visually depict the spatial arrangement of this vector, assigning the same value to all vertices within each parcel. Notably, the data used to infer the HMM were standardized to ensure a zero mean and unit standard deviation across time for each parcel. Consequently, an activation level of zero corresponds to the mean activation of the respective parcel. Negative activations (depicted in cool colors) indicate relatively subdued BOLD activity (i.e., below average), while positive activations (shown in warm colors) denote heightened BOLD activity (i.e., above average).

To clarify which resting state network (RSN) most defines each hidden state, we computed a summary measure for each hemisphere and RSN. This measure quantifies the extent of deviation of each RSN from the average level of activation. In our visualization (Fig. 2), warmer colors represent higher positive deviations from the mean, while cooler colors represent higher negative deviations from the mean. Among all brain states, states 2 and 4 stand as the primary extremes: the former exhibits generally low mean activation, while the latter displays high activation primarily within unimodal and attentional networks. Additionally, state 1 showcases elevated activation mainly in regions belonging to the somatomotor network, while state 6 manifests heightened activation in visual and frontal regions. The remaining states predominantly feature activation in multimodal regions, including the default mode network (DMN) in state 3, the dorsal attentional network in state 5, and a combination of the ventral attentional network and DMN in state 7.

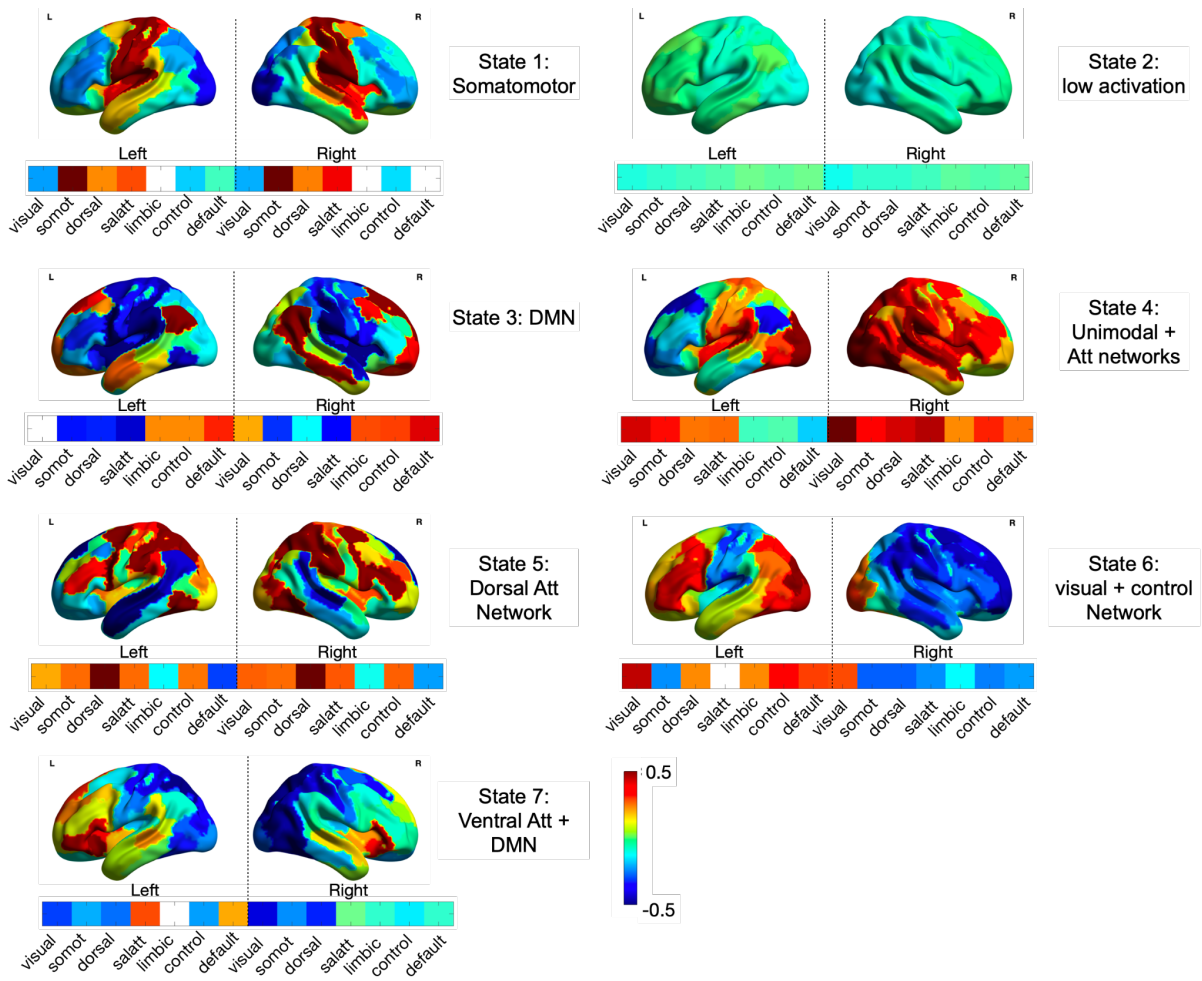

Figure 2. States characterization. Whole brain mean activation maps represented on the brain surface and as deviation from the mean activation. Lateral brain surface where each parcel is color-coded according to the activation extracted when the specific state is active. On the bottom of each brain surface we present the percentage of deviation from the mean level of activation for each resting state network and hemisphere (RSN order: visual, somatomotor, dorsal attentional, salience, limbic, control and default mode network). Warm colors indicate activations higher than the mean; cold colors indicate activations lower than the mean.

Altered dynamics in blindness

We conducted between-group comparisons on three pivotal metrics defining the *chronnectome*: 1) Fractional Occupancy (FO), indicating the proportion of time spent visiting a state; 2) Mean Lifetime, denoting the number of timepoints per visit; and 3) Switching Rate (SR), representing the frequency of transitions between states. In Fig. 3, we present the results for all metrics.

Significant disparities emerged in Fractional Occupancy (Fig. 3, panel A), with blind people showing a propensity to visit states 1 and 6 more frequently, whereas controls exhibited a higher propensity to visit state 7 (FDR-p=0.004). It's crucial to contextualize these findings within the characterization of the states to glean deeper insights. States 1 and 6 primarily exhibit activation in unimodal regions, with state 1 showing heightened activity in somatomotor regions and state 6 in visual areas. Furthermore, state 6 entails activation of regions within the Default Mode and Control networks, predominantly lateralized to the left hemisphere. In contrast, controls tend to favor state 7, characterized by activation

in regions of the Default Mode and Ventral Attentional networks, devoid of involvement from unimodal regions. Upon conducting separate analyses on the two datasets, we observed similar results (see Fig. S3), confirming that these primary findings exhibit robustness across datasets. In addition, we observed a discrepancy in state 3 (FDR-p = 0.009), wherein controls displayed higher Fractional Occupancy when analyzing the dataset1. Interestingly, in 2 out of 3 states in which we did not find any significant between group difference (state 4 FDR-p = 0.51 - state 5 FDR-p = 0.16), we observe a clear activation of bilateral occipital areas, together with unimodal and multimodal regions.

No significant disparities were detected in the mean lifetime metric (Fig. 3, panel B), suggesting that both groups allocated a similar number of timepoints per visit, irrespective of differences in Fractional Occupancy. This implies that even in states exhibiting higher Fractional Occupancy in either blind or sighted individuals, the average duration of each visit remained consistent across groups. Upon conducting separate analyses on the two datasets, we observed congruent results (see Fig. S3), with the sole exception of a notable difference in state 3 (FDR-p = 0.006) when analyzing the dataset1, indicating a longer visit duration in sighted compared to blind individuals.

We did not find any difference in terms of switching rate (FDR-p=0.115), with blind and sighted individuals switching among states every 0.169Hz (5.91 seconds) and 0.167Hz (5.98 seconds) respectively (Fig. 03, panel D). The examination of the switching rate trend across subjects (Fig. 3, panel C) revealed generally higher values in the first than in the second dataset, as well as a bigger between-group difference when considering only the first dataset. Indeed, upon conducting separate analyses on the two datasets, we observed a significant difference only when considering the dataset1, with significantly higher switching rate in blind (0.209Hz) than sighted individuals (0.185Hz - FDR-p = 0.027). Thus, any potential between-group differences in this regard may be attributed more to sample characteristics or scanner type rather than early visual deprivation.

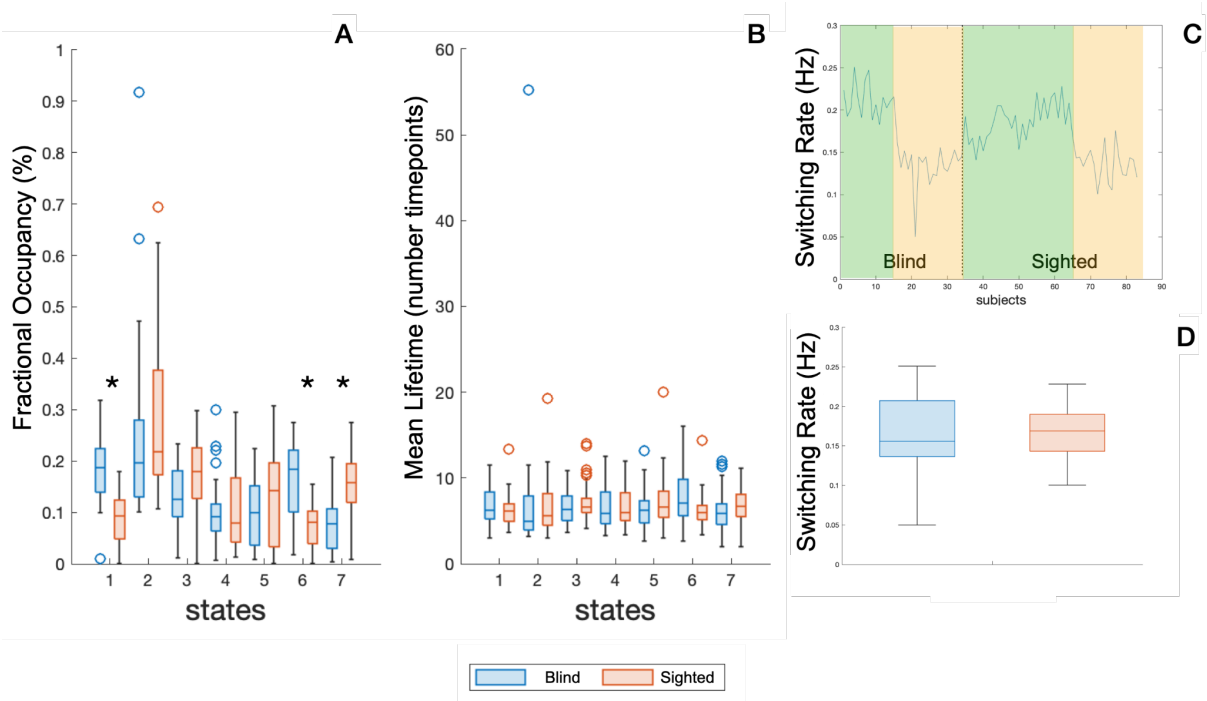

Figure 3. Differences in the *chronnectome* between blind and sighted individuals. A: Fractional Occupancy for each group, as a function of state. B: Mean Lifetime for each group, as a function of state. C: Switching rate (Hz) for each subject (upper), with green background indicating subjects belonging to dataset1 and orange background indicating subjects belonging to the dataset2, and for each group (bottom). Significant results after FDR correction are highlighted with *.

Stability in the chronnectome

In our analysis, we explored various model orders ranging from 5 to 9 states, as detailed previously (Fig. 4). Interestingly, consistent findings emerged when evaluating between-group disparities in Fractional Occupancy (FO). Particularly noteworthy was the most consistent results across models, represented by a heightened FO observed in blind individuals within a state marked by bilateral somatomotor and auditory region activation. Moreover, blind people exhibited elevated FO in states featuring robust activation of the visual network, often in conjunction with fronto-parietal regions. Conversely, controls tended to display higher FO in states characterized by multimodal region activation and cortical hubs, notably regions associated with the Default Mode Network. These findings highlight that our conclusions are not purely driven by the order chosen.

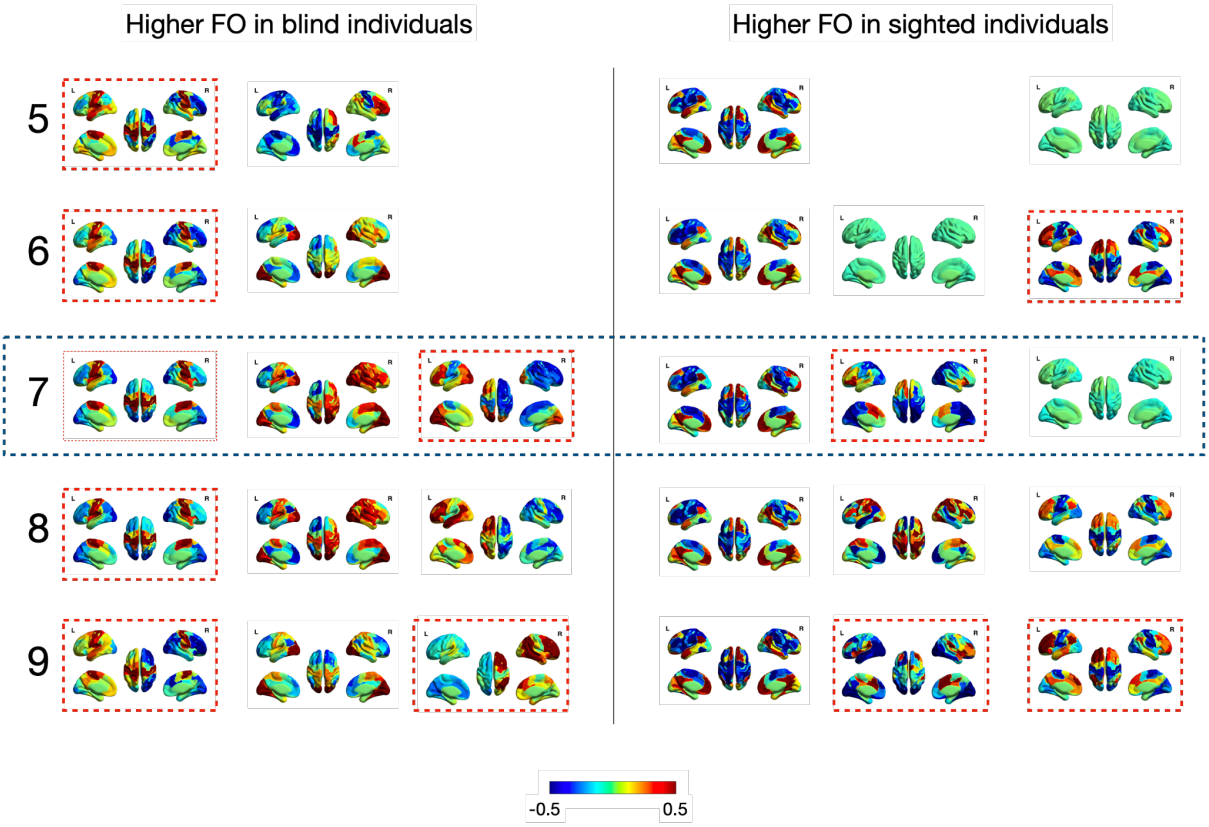

Figure 4. Maps of mean activation estimated from HMM using different numbers of states (from 5 to 9). Dashed red squares indicate significant results. The blue dashed square indicates the chosen model order.

Transition Probabilities

An additional feature of the Chronnectome is represented by the matrix of transition probability (K x K matrices, where K is the number of states). We extracted these matrices at subject level, excluding probabilities of persistence (diagonal of the matrix), by using the function *getTransProbs* of the HMM-MAR toolbox, and computed the median values separately for blind and sighted individuals (see Fig. 5A). Fig.5B illustrates the hierarchical clustering (using Ward's algorithm) on the resulting transition probability matrices, for blind (top) and sighted (bottom) individuals.

Remarkably, both groups exhibited similar patterns, with a heightened probability of transitioning from any state to state 2, characterized by overall low activation levels across the entire brain, closely approximating the mean. In addition to this overarching trend, when considering the top 20% highest probabilities in both groups, notable distinctions emerge (see Fig. 5C). Blind people displayed a greater likelihood of transitioning from state 7 or 3 to state 1, whereas controls exhibited a higher probability of transitioning from state 2 to either state 3 or state 7 and from states 6 or 5 to state 3. These findings align well with the previously observed patterns of higher FO in blind subjects in state 1 and higher FO in sighted in states 3 and 7.

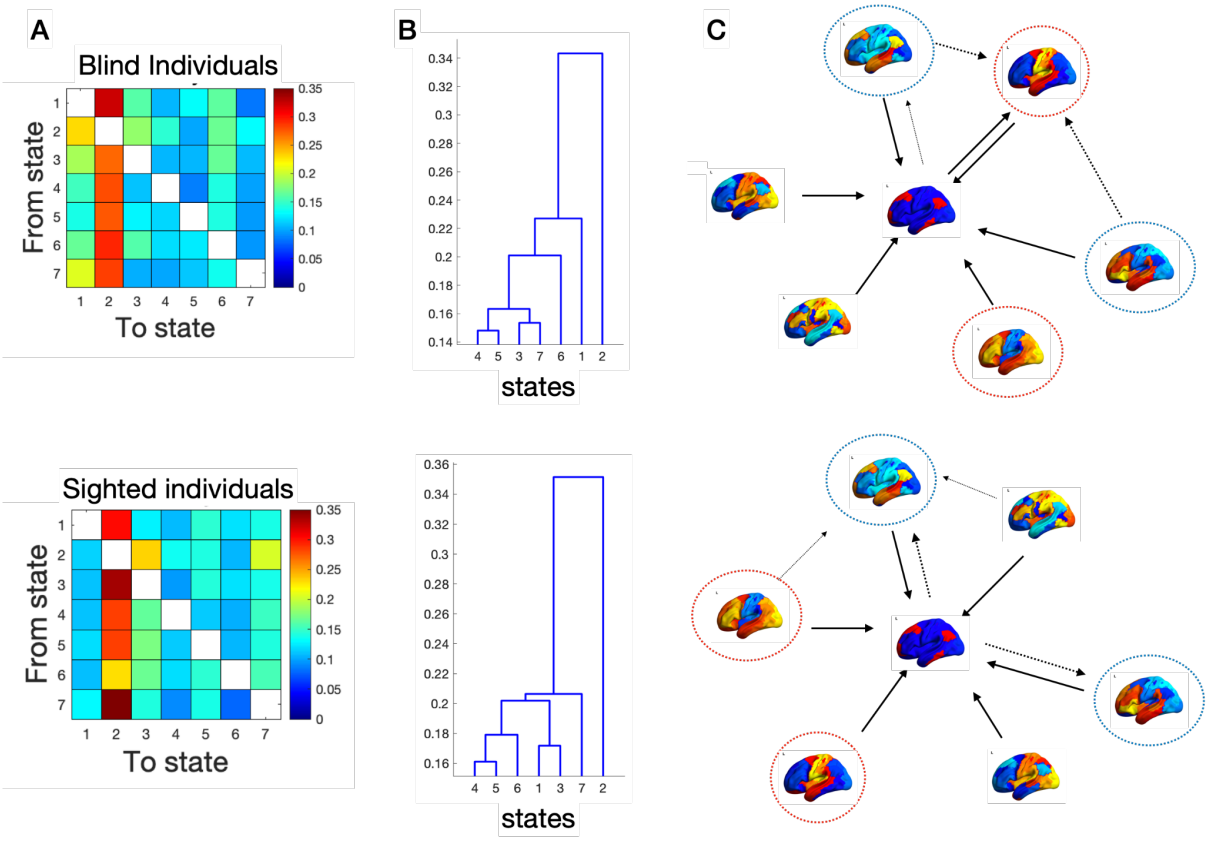

Figure 5. Transition probability matrices in blind and sighted individuals. A. Median transition probability matrices for blind (top) and sighted (bottom) individuals. B. Dendrogram showing the clusters of states based on the median transition probabilities. C. Graph showing the 20% higher probabilities between states.

Functional connectivity

In this study, we considered two FC-related representations of the data at subject level: a time-averaged functional connectome and a time-varying functional connectome when each state is active. Our results on stationary resting-state functional connectivity (rs-FC) align with previous findings (Burton et al., 2014; Guerreiro et al., 2021; Koba et al., 2024; Rączy et al., 2022; Tian et al., 2024), showing a general trend of reduced rs-FC between visual and somatomotor regions and increased rs-FC between visual and prefrontal regions in individuals with blindness. Additionally, we observed an increase in rs-FC in blind individuals between visual areas and either the bilateral precuneus (part of the DMN) or the temporal fusiform cortex (see Figure 6B).

When analyzing the time-varying functional connectome, we identified clear differences among states. In 4 out of 7 states, blind subjects exhibited reduced functional connectivity between visual and somatomotor regions compared to controls. These differences were more pronounced in states with higher FO in controls (states 3 and 7) and in state 2 (Fig. S4), which was characterized by low mean activation but slightly elevated connectivity in the Default Mode and Control Networks. Conversely, in 2 out of 7 states (states 1 and 5), we observed enhanced rs-FC between visual areas and the bilateral temporal fusiform cortex, corresponding to the parcel Vis1 in the Schaefer Atlas (Fig. 6 and S4).

Notably, state 1 showed higher FO in blind than in sighted people. Additionally, only one state (6), which was more frequently occupied by blind individuals, displayed increased rs-FC between visual and right prefrontal regions, indicating heightened inter-network coupling. It is important to notice that states 1, 5 and 6, which are associated with higher rs-FC in blind individuals, align with the increased rs-FC observed in the stationary FC analysis. Conversely, states 2, 3 and 7, which show higher FO in controls, align with the higher rs-FC observed in controls in the stationary FC analysis. These findings suggest that differences identified by stationary FC analysis may result not only from changes in rs-FC but also from variations in the time spent visiting a specific state.

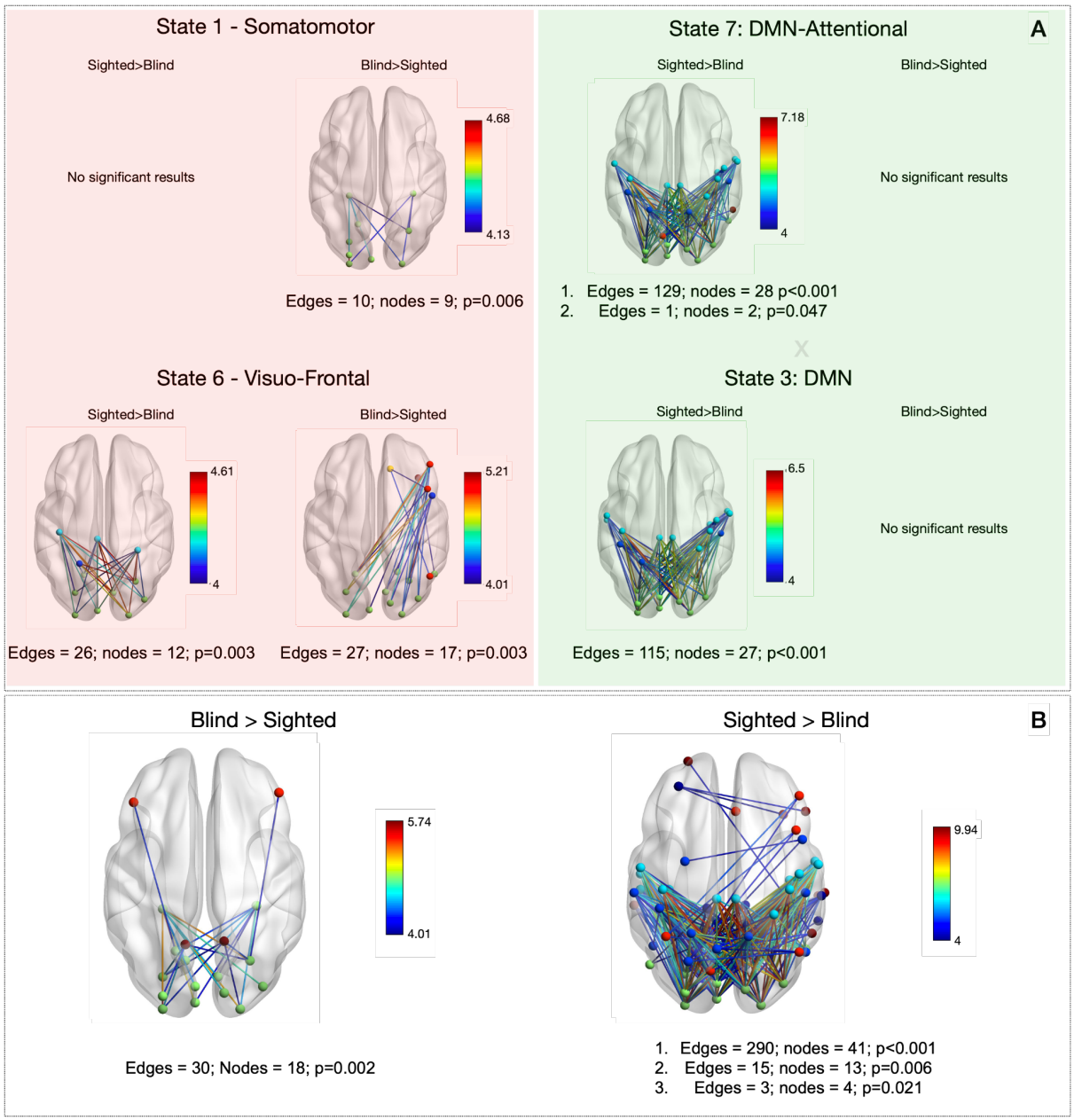

Figure 6. Network-level between-group analysis. Between-group differences in the functional connectome for the time-varying FC (A) and the stationary FC (B). The red background indicates states with FO higher in blind individuals; the green background indicates states with FO higher in controls.

Discussion

Early blindness alters the structural and functional architecture of the brain. Alterations in the functional connectome have been observed (Burton et al., 2014; Guerreiro et al., 2021; Koba et al., 2024; Ortiz-Terán et al., 2016), with most research traditionally emphasizing the static characterization of connectivity. Conversely, in this study we assessed whether the absence of vision during the early period of visual development could lead to changes in the temporal dynamics of functional connectivity (FC) states.

From the perspective of dynamical systems theory, the brain can be understood as a system composed of various 'attractors', that are stable patterns of neural activity where brain states temporarily settle. Switching between these brain states define the multi-stable feature of the system that never settles in a single state (Deco & Jirsa, 2012). Computational models of whole brain network dynamics, based on tractography-derived realistic connectivity, suggest that resting-state activity operates at a critical bifurcation point on the edge of instability, exploring a variety of brain states (Breakspear, 2017; Cabral et al., 2014; Deco & Jirsa, 2012; Hansen et al., 2015).

Minor changes in the system's properties, such as shifts in the excitatory/inhibitory (E/I) balance, can impact the overall dynamics, leading to alterations in temporal dynamics (Hansen et al., 2015; Nakagawa et al., 2013). Early sensory deprivation has been shown to trigger a disruption of the E/I balance between crossmodal brain regions (Gainey & Feldman, 2017; Muret & Makin, 2021), leading to Hebbian and/or homeostatic plasticity mechanisms (Gainey & Feldman, 2017). This may result in heightened activation of occipital regions, facilitating cross-modal plasticity (Kral et al., 2017). This hypothesis resonates well with the evidence from M/EEG studies in early blind populations, where occipital alpha oscillations (inhibitory feedback processing) are reduced while posterior gamma rhythms (feedforward processing) are increased in congenitally blind individuals (Kriegseis et al., 2006; Lubinus et al., 2021; Pant et al., 2023). Recently (Rączy et al., 2022) explored the E/I balance by analyzing the amplitude of low frequency fluctuation (ALFF) of the blood oxygen level-dependent (BOLD) signal in congenitally blind individuals. They reported higher ALFF in occipital regions that reflect higher resting-state excitatory activity of less pruned neural circuits, possibly highlighting an E/I imbalance following early deprivation.

Following early visual deprivation, the disruption of the E/I balance may lead to subtle changes in the system's properties, affecting the temporal dynamics of brain states. In this study, we applied a data-driven approach using Hidden Markov Models (HMM) to analyze the concatenated time courses of early blind individuals and sighted controls, aiming to assess alterations in the temporal dynamics of the functional connectome over time (chronnectome).

We observed significant differences in the frequency of occupying specific brain states, as reflected in the fractional occupancy. Interestingly, despite these differences, the overall switching rate between

states was similar across groups, suggesting that early sensory deprivation does not alter the multi-stability feature of the system. Specifically, three states were more frequently occupied by either blind or sighted individuals, suggesting that the frequency of visiting FC states may serve as a distinguishing feature between the two groups.

Blind individuals tended to visit more frequently two states characterized by the cross-talk between non-deprived (auditory/somatomotor) sensory regions, as well as between deprived sensory (occipital) and frontal regions. In contrast, controls more frequently visited a state characterized by the activation of regions belonging to the Default Mode and Ventral Attentional networks, without involving unimodal regions. The increased frequency of visiting states involving unimodal and frontal regions might represent the baseline brain state fluctuations leading to the increased activation of either deprived (occipital) or not-deprived unimodal regions during sensory and cognitive tasks following visual deprivation (Amedi et al., 2003, 2004; Bedny et al., 2011; Collignon et al., 2013; Gagnon et al., 2015; Gougoux et al., 2009; Noppeney, 2007; Raz et al., 2005). Specifically, the increased occupancy of bilateral somatomotor regions may be linked to the different tactile and body-related abilities (Radziun et al., 2023) reported in early blind individuals. This suggests that non-deprived unimodal regions might play a significant role in body awareness, extending beyond the previously established link between body awareness and structural changes in the occipital cortex (Stroh et al., 2024).

In addition to the map of mean activation, each brain state is characterized by a functional connectome that captures the correlation between brain regions when a specific state is active. Based on the observed differences in the proportion of time spent visiting various states, we investigated potential alterations in the functional connectome following visual deprivation.

In brain states more frequently occupied by sighted individuals—marked by high activation of regions in the Default Mode and Attentional Networks—we observed decreased functional connectivity between visual and auditory/somatomotor regions in blind individuals. This pattern was confirmed by stationary functional connectivity analysis, consistent with prior findings (Burton et al., 2014; Guerreiro et al., 2021; Koba et al., 2024; Tian et al., 2024). Notably, one of the main regions activated in this state is the medial prefrontal cortex (mPFC), a core region of the Default Mode Network (DMN) (Fox & Raichle, 2007). Previous studies suggest that the mPFC plays a key role in generating mental imagery (Amedi et al., 2005), a cognitive process grounded in sensory properties that involves both primary sensory and higher-order brain regions (Bergmann et al., 2016; Daselaar et al., 2010; Zhang et al., 2018). Based on our results, we speculate that the activation of mPFC, along with increased connectivity between sensory regions, may be linked to visual imagery of body parts or motor actions. Interestingly, the observed higher connectivity between visual and auditory/somatomotor regions in sighted individuals at rest suggests that occipital region connectivity is task-dependent. Indeed, external non-visual stimuli during sensory tasks may inhibit occipital regions, reducing connectivity between

unimodal regions in sighted participants, while at rest this connectivity remains higher. However, in cases of sensory deprivation, the E/I imbalance might reverse this pattern, resulting in lower connectivity between visual and auditory/somatomotor regions at rest and higher connectivity during a sensory task (Pelland et al., 2017).

In states where blind individuals showed higher fractional occupancy, the pattern of between-group differences in the functional connectome varied. For instance, in the state characterized by bilateral somatomotor activation, we observed increased resting-state functional connectivity in blind individuals within the visual network, connecting multiple occipital regions with the bilateral temporal fusiform cortex. This pattern also emerged from the stationary functional connectivity analysis and represents a novel finding, contrasting with previous studies that typically report decreased connectivity within the sensory-deprived network (Liu et al., 2007; Qin et al., 2015). These results may support cross-modal plasticity in two key ways. First, they suggest that cross-modal plasticity may be facilitated by strengthened intra-visual cortex connections (Burton et al., 2014). Second, the combination of heightened activation in bilateral somatomotor regions and increased connectivity within the visual network may establish functional links between sensory-deprived and non-deprived unimodal regions.

Blind individuals also spend more time in a state characterized by visuo-frontal activation and increased functional connectivity between visual and prefrontal regions. The co-activation of frontal and occipital region, together with their increased FC, align with previous findings showing an increased interaction between occipital regions and higher-cognitive networks of frontoparietal cortices, including networks that support language, numerical cognition, executive control and working memory (Bedny, 2017; Bedny et al., 2011; Deen et al., 2015). These findings support the hypothesis proposed by (Pelland et al., 2017) that the occipital cortex exhibits features of a multiple-demand (MD) system (Duncan, 2010), which involves regions that are not specific to any particular stimuli, modality, or task. The stronger coupling with frontal regions, likely belonging to the MD system, may confirm the involvement of occipital regions in the MD system.

Together, these findings indicate that early visual deprivation results in specific alterations in the brain's FC patterns, particularly affecting the visual network and its interactions with other sensory and frontal regions. Additionally, our results suggest that differences observed in stationary rs-FC may stem not only from changes in connectivity itself but also from variations in the time spent in specific brain states, highlighting that differences in the functional connectome might result from alterations in the temporal dynamics of functional connectivity of brain states.

Future research could benefit from validating these findings with larger samples or optimized acquisition protocols that allow for the application of Hidden Markov Models (HMM) without

dimensionality reduction. Indeed, recent studies showed that the dimensionality reduction performed through PCA can lead to spurious oscillatory patterns called 'phantom oscillations' that can affect the data analysis (Shinn, 2023). Additionally, investigating the temporal dynamics of functional connectivity in late-blind individuals, as well as in those undergoing sight recovery, represents a promising research avenue. It would be particularly interesting to test whether: 1) similar alterations in temporal dynamics are observed even when visual deprivation occurs after the closure of the sensitive period of development, and 2) these alterations are reversed following sight restoration happening either before or after the closure of the sensitive period. Given the growing interest in structural-functional coupling (SFC) quantifying how strongly brain structure shapes and constraints function (Fotiadis et al., 2023, 2024), the use of HMM could provide valuable insights into how structural changes influence dFC following sensory deprivation. Implementing a state-specific functional connectome could allow us to test the temporal dynamics of SFC and its alterations following visual deprivation.

Limitations

This study is not exempt from limitations strictly related to the method used. Indeed, the data-driven approach of HMM has an intrinsic limitation represented by the choice of the number of brain states as a priori decision that needs to be made to fit the model. Although we attempted to optimize the process of model order decision and compared results obtained from different model orders, it is important to acknowledge this as a limitation of the study. Furthermore, the concatenation of the timecourses to estimate the parameters implicitly forces the model to estimate the same brain states for all subjects, potentially masking between-group differences in brain states. While the same method could be used to estimate states from the data of each group (blind or sighted), this would not allow for a direct statistical comparison between the metrics of the two groups, as performed in our study. We addressed this limitation by inspecting the Gamma signal at subject level and ensuring that each state is visited by both groups, thus ruling out the possibility that one state clearly describes only one group.

Conclusions

Our findings highlight the utility of Hidden Markov Models (HMM) in capturing the temporal dynamics of functional connectivity and its alterations following sensory deprivation. Specifically, we observed significant disruptions in these dynamics due to early visual deprivation. Blindness resulted in prolonged occupancy in brain states that primarily activate unimodal regions, with increased connectivity involving occipital regions. Additionally, our results suggest that changes in the chronnectome—particularly the time spent in specific states—may offer insights into the patterns of stationary functional connectivity following sensory deprivation, notably the unexpected reduction in connectivity between occipital and sensorimotor regions.

Data, Materials, and Software Availability

Anonymized neuroimaging data as well as codes used to estimate the HMM, compare the model orders and run the statistical analysis have been deposited in the Open Science Framework (https://osf.io/8a7ft/).

References

Abboud, S., & Cohen, L. (2019). Distinctive Interaction Between Cognitive Networks and the Visual Cortex in Early Blind Individuals. *Cerebral Cortex* , *29*(11), 4725–4742.

Amedi, A., Floel, A., Knecht, S., Zohary, E., & Cohen, L. G. (2004). Transcranial magnetic stimulation of the occipital pole interferes with verbal processing in blind subjects. *Nature Neuroscience*, *7*(11), 1266–1270.

Amedi, A., Malach, R., & Pascual-Leone, A. (2005). Negative BOLD differentiates visual imagery and perception. *Neuron*, *48*(5), 859–872.

Amedi, A., Raz, N., Pianka, P., Malach, R., & Zohary, E. (2003). Early "visual" cortex activation correlates with superior verbal memory performance in the blind. *Nature Neuroscience*, *6*(7), 758–766.

Baker, A. P., Brookes, M. J., Rezek, I. A., Smith, S. M., Behrens, T., Probert Smith, P. J., & Woolrich, M. (2014). Fast transient networks in spontaneous human brain activity. *eLife*, *3*, e01867.

Bauer, C. M., Hirsch, G. V., Zajac, L., Koo, B.-B., Collignon, O., & Merabet, L. B. (2017). Multimodal MR-imaging reveals large-scale structural and functional connectivity changes in profound early blindness. *PloS One*, *12*(3), e0173064.

Bedny, M. (2017). Evidence from Blindness for a Cognitively Pluripotent Cortex. *Trends in Cognitive Sciences*, *21*(9), 637–648.

Bedny, M., Pascual-Leone, A., Dodell-Feder, D., Fedorenko, E., & Saxe, R. (2011). Language processing in the occipital cortex of congenitally blind adults. *Proceedings of the National Academy of Sciences of the United States of America*, *108*(11), 4429–4434.

Beer, A. L., Plank, T., & Greenlee, M. W. (2011). Diffusion tensor imaging shows white matter tracts between human auditory and visual cortex. *Experimental Brain Research*, *213*(2-3), 299–308.

Bergmann, J., Genç, E., Kohler, A., Singer, W., & Pearson, J. (2016). Smaller primary visual cortex is associated with stronger, but less precise mental imagery. *Cerebral Cortex (New York, N.Y.: 1991)*, *26*(9), 3838–3850.

Bock, A. S., & Fine, I. (2014). Anatomical and functional plasticity in early blind individuals and the mixture of experts architecture. *Frontiers in Human Neuroscience*, *8*, 971.

Breakspear, M. (2017). Dynamic models of large-scale brain activity. *Nature Neuroscience*, *20*(3), 340–352.

Burton, H., Snyder, A. Z., & Raichle, M. E. (2014). Resting state functional connectivity in early blind humans. *Frontiers in Systems Neuroscience*, *8*, 51.

Cabral, J., Kringelbach, M. L., & Deco, G. (2014). Exploring the network dynamics underlying brain activity during rest. *Progress in Neurobiology*, *114*, 102–131.

Cao, B., Chen, Y., Yu, R., Chen, L., Chen, P., Weng, Y., Chen, Q., Song, J., Xie, Q., & Huang, R. (2019). Abnormal dynamic properties of functional connectivity in disorders of consciousness. *NeuroImage. Clinical*, *24*, 102071.

Carbo, E. W. S., Hillebrand, A., van Dellen, E., Tewarie, P., de Witt Hamer, P. C., Baayen, J. C., Klein, M., Geurts, J. J. G., Reijneveld, J. C., Stam, C. J., & Douw, L. (2017). Dynamic hub load predicts cognitive decline after resective neurosurgery. *Scientific Reports*, *7*, 42117.

Cohen, L. G., Celnik, P., Pascual-Leone, A., Corwell, B., Falz, L., Dambrosia, J., Honda, M., Sadato, N., Gerloff, C., Catalá, M. D., & Hallett, M. (1997). Functional relevance of cross-modal plasticity in blind humans. *Nature*, *389*(6647), 180–183.

Collignon, O., Davare, M., Olivier, E., & De Volder, A. G. (2009). Reorganisation of the right occipito-parietal stream for auditory spatial processing in early blind humans. A transcranial magnetic stimulation study. *Brain Topography*, *21*(3-4), 232–240.

Collignon, O., Dormal, G., Albouy, G., Vandewalle, G., Voss, P., Phillips, C., & Lepore, F. (2013). Impact of blindness onset on the functional organization and the connectivity of the occipital cortex. *Brain: A Journal of Neurology*, *136*(Pt 9), 2769–2783.

Collignon, O., Lassonde, M., Lepore, F., Bastien, D., & Veraart, C. (2006). Functional cerebral reorganization for auditory spatial processing and auditory substitution of vision in early blind subjects. *Cerebral Cortex (New York, N.Y.: 1991)*, *17*(2), 457–465.

Collignon, O., Vandewalle, G., Voss, P., Albouy, G., Charbonneau, G., Lassonde, M., & Lepore, F. (2011). Functional specialization for auditory–spatial processing in the occipital cortex of congenitally blind humans. *Proceedings of the National Academy of Sciences*, *108*(11), 4435–4440.

Collignon, O., Voss, P., Lassonde, M., & Lepore, F. (2009). Cross-modal plasticity for the spatial processing of sounds in visually deprived subjects. *Experimental Brain Research. Experimentelle Hirnforschung. Experimentation Cerebrale*, *192*(3), 343–358.

Damaraju, E., Allen, E. A., Belger, A., Ford, J. M., McEwen, S., Mathalon, D. H., Mueller, B. A., Pearlson, G. D., Potkin, S. G., Preda, A., Turner, J. A., Vaidya, J. G., van Erp, T. G., & Calhoun, V. D. (2014). Dynamic functional connectivity analysis reveals transient states of dysconnectivity in schizophrenia. *NeuroImage. Clinical*, *5*, 298–308.

Daselaar, S. M., Porat, Y., Huijbers, W., & Pennartz, C. M. A. (2010). Modality-specific and modality-independent components of the human imagery system. *NeuroImage*, *52*(2), 677–685.

Deco, G., & Jirsa, V. K. (2012). Ongoing cortical activity at rest: criticality, multistability, and ghost attractors. *The Journal of Neuroscience: The Official Journal of the Society for Neuroscience*, *32*(10), 3366–3375.

Deco, G., Jirsa, V. K., & McIntosh, A. R. (2011). Emerging concepts for the dynamical organization of resting-state activity in the brain.

Nature Reviews. Neuroscience, *12*(1), 43–56.

Deen, B., Saxe, R., & Bedny, M. (2015). Occipital cortex of blind individuals is functionally coupled with executive control areas of frontal cortex. *Journal of Cognitive Neuroscience*, *27*(8), 1633–1647.

Dormal, G., & Collignon, O. (2011). Functional selectivity in sensory-deprived cortices. *Journal of Neurophysiology*, *105*(6), 2627–2630.

Duncan, J. (2010). The multiple-demand (MD) system of the primate brain: mental programs for intelligent behaviour. *Trends in Cognitive Sciences*, *14*(4), 172–179.

Elbert, T., Sterr, A., Rockstroh, B., Pantev, C., Müller, M. M., & Taub, E. (2002). Expansion of the tonotopic area in the auditory cortex of the blind. *The Journal of Neuroscience: The Official Journal of the Society for Neuroscience*, *22*(22), 9941–9944.

Esteban, O., Markiewicz, C. J., Blair, R. W., Moodie, C. A., Isik, A. I., Erramuzpe, A., Kent, J. D., Goncalves, M., DuPre, E., Snyder, M., Oya, H., Ghosh, S. S., Wright, J., Durnez, J., Poldrack, R. A., & Gorgolewski, K. J. (2019). fMRIPrep: a robust preprocessing pipeline for functional MRI. *Nature Methods*, *16*(1), 111–116.

Falchier, A., Clavagnier, S., Barone, P., & Kennedy, H. (2002). Anatomical evidence of multimodal integration in primate striate cortex. *The Journal of Neuroscience: The Official Journal of the Society for Neuroscience*, *22*(13), 5749–5759.

Fotiadis, P., Cieslak, M., He, X., Caciagli, L., Ouellet, M., Satterthwaite, T. D., Shinohara, R. T., & Bassett, D. S. (2023). Myelination and excitation-inhibition balance synergistically shape structure-function coupling across the human cortex. *Nature Communications*, *14*(1), 6115.

Fotiadis, P., Parkes, L., Davis, K. A., Satterthwaite, T. D., Shinohara, R. T., & Bassett, D. S. (2024). Structure-function coupling in macroscale human brain networks. *Nature Reviews. Neuroscience*. https://doi.org/10.1038/s41583-024-00846-6

Fox, M. D., & Raichle, M. E. (2007). Spontaneous fluctuations in brain activity observed with functional magnetic resonance imaging. *Nature Reviews. Neuroscience*, *8*(9), 700–711.

Frasnelli, J., Collignon, O., Voss, P., & Lepore, F. (2011). Crossmodal plasticity in sensory loss. *Progress in Brain Research*, *191*, 233–249.

Friston, K. J. (1994). Functional and effective connectivity in neuroimaging: A synthesis. *Human Brain Mapping*, *2*(1-2), 56–78.

Friston, K. J., Harrison, L., & Penny, W. (2003). Dynamic causal modelling. *NeuroImage*, *19*(4), 1273–1302.

Gagnon, L., Kupers, R., & Ptito, M. (2015). Neural correlates of taste perception in congenital blindness. *Neuropsychologia*, *70*, 227–234.

Gainey, M. A., & Feldman, D. E. (2017). Multiple shared mechanisms for homeostatic plasticity in rodent somatosensory and visual cortex. *Philosophical Transactions of the Royal Society of London. Series B, Biological Sciences*, *372*(1715). https://doi.org/10.1098/rstb.2016.0157

Gorgolewski, K. J., Alfaro-Almagro, F., Auer, T., Bellec, P., Capotă, M., Chakravarty, M. M., Churchill, N. W., Cohen, A. L., Craddock, R. C., Devenyi, G. A., Eklund, A., Esteban, O., Flandin, G., Ghosh, S. S., Guntupalli, J. S., Jenkinson, M., Keshavan, A., Kiar, G., Liem, F., … Poldrack, R. A. (2017). BIDS apps: Improving ease of use, accessibility, and reproducibility of neuroimaging data analysis methods. *PLoS Computational Biology*, *13*(3), e1005209.

Gougoux, F., Belin, P., Voss, P., Lepore, F., Lassonde, M., & Zatorre, R. J. (2009). Voice perception in blind persons: a functional magnetic resonance imaging study. *Neuropsychologia*, *47*(13), 2967–2974.

Griffanti, L., Salimi-Khorshidi, G., Beckmann, C. F., Auerbach, E. J., Douaud, G., Sexton, C. E., Zsoldos, E., Ebmeier, K. P., Filippini, N., Mackay, C. E., Moeller, S., Xu, J., Yacoub, E., Baselli, G., Ugurbil, K., Miller, K. L., & Smith, S. M. (2014). ICA-based artefact removal and accelerated fMRI acquisition for improved resting state network imaging. *NeuroImage*, *95*, 232–247.

Guerreiro, M. J. S., Linke, M., Lingareddy, S., Kekunnaya, R., & Röder, B. (2021). The effect of congenital blindness on resting-state functional connectivity revisited. *Scientific Reports*, *11*(1), 1–14.

Hansen, E. C. A., Battaglia, D., Spiegler, A., Deco, G., & Jirsa, V. K. (2015). Functional connectivity dynamics: modeling the switching behavior of the resting state. *NeuroImage*, *105*, 525–535.

Hertrich, I., Dietrich, S., & Ackermann, H. (2013). Tracking the speech signal--time-locked MEG signals during perception of ultra-fast and moderately fast speech in blind and in sighted listeners. *Brain and Language*, *124*(1), 9–21.

Hutchison, R. M., Womelsdorf, T., Allen, E. A., Bandettini, P. A., Calhoun, V. D., Corbetta, M., Della Penna, S., Duyn, J. H., Glover, G. H., Gonzalez-Castillo, J., Handwerker, D. A., Keilholz, S., Kiviniemi, V., Leopold, D. A., de Pasquale, F., Sporns, O., Walter, M., & Chang, C. (2013). Dynamic functional connectivity: promise, issues, and interpretations. *NeuroImage*, *80*, 360–378.

Kim, J., Criaud, M., Cho, S. S., Díez-Cirarda, M., Mihaescu, A., Coakeley, S., Ghadery, C., Valli, M., Jacobs, M. F., Houle, S., & Strafella, A. P. (2017). Abnormal intrinsic brain functional network dynamics in Parkinson's disease. *Brain: A Journal of Neurology*, *140*(11), 2955–2967.

Klinge, C., Eippert, F., Röder, B., & Büchel, C. (2010). Corticocortical connections mediate primary visual cortex responses to auditory stimulation in the blind. *The Journal of Neuroscience: The Official Journal of the Society for Neuroscience*, *30*(38), 12798–12805.

Koba, C., Crimi, A., Collignon, O., Ricciardi, E., & Hasson, U. (2024). Neural networks associated with eye movements in congenital blindness. *The European Journal of Neuroscience*. https://doi.org/10.1111/ejn.16459

Kottaram, A., Johnston, L. A., Cocchi, L., Ganella, E. P., Everall, I., Pantelis, C., Kotagiri, R., & Zalesky, A. (2019). Brain network dynamics in schizophrenia: Reduced dynamism of the default mode network. *Human Brain Mapping*, *40*(7), 2212–2228.

Kral, A., Yusuf, P. A., & Land, R. (2017). Higher-order auditory areas in congenital deafness: Top-down interactions and corticocortical decoupling. *Hearing Research*, *343*, 50–63.

Kriegseis, A., Hennighausen, E., Rösler, F., & Röder, B. (2006). Reduced EEG alpha activity over parieto-occipital brain areas in congenitally blind adults. *Clinical Neurophysiology: Official Journal of the International Federation of Clinical Neurophysiology*, *117*(7), 1560–1573.

Kucyi, A., Hove, M. J., Esterman, M., Hutchison, R. M., & Valera, E. M. (2017). Dynamic brain network correlates of spontaneous fluctuations in attention. *Cerebral Cortex (New York, N.Y.: 1991)*, *27*(3), 1831–1840.

Leclerc, C., Saint-Amour, D., Lavoie, M. E., Lassonde, M., & Lepore, F. (2000). Brain functional reorganization in early blind humans revealed by auditory event-related potentials. *Neuroreport*, *11*(3), 545–550.

Liu, Y., Yu, C., Liang, M., Li, J., Tian, L., Zhou, Y., Qin, W., Li, K., & Jiang, T. (2007). Whole brain functional connectivity in the early blind. *Brain: A Journal of Neurology*, *130*(Pt 8), 2085–2096.

Li, X., Morgan, P. S., Ashburner, J., Smith, J., & Rorden, C. (2016). The first step for neuroimaging data analysis: DICOM to NIfTI

conversion. *Journal of Neuroscience Methods*, *264*, 47–56.

Lubinus, C., Orpella, J., Keitel, A., Gudi-Mindermann, H., Engel, A. K., Roeder, B., & Rimmele, J. M. (2021). Data-Driven Classification of Spectral Profiles Reveals Brain Region-Specific Plasticity in Blindness. *Cerebral Cortex* , *31*(5), 2505–2522.

Makin, T. R., & Krakauer, J. W. (2023). Against cortical reorganisation. *eLife*, *12*. https://doi.org/10.7554/eLife.84716

Mattioni, S., Rezk, M., Battal, C., Bottini, R., Cuculiza Mendoza, K. E., Oosterhof, N. N., & Collignon, O. (2020). Categorical representation from sound and sight in the ventral occipito-temporal cortex of sighted and blind. *eLife*, *9*. https://doi.org/10.7554/eLife.50732

Menon, S. S., & Krishnamurthy, K. (2019). A Comparison of Static and Dynamic Functional Connectivities for Identifying Subjects and Biological Sex Using Intrinsic Individual Brain Connectivity. *Scientific Reports*, *9*(1), 5729.

Moretto, M., Silvestri, E., Facchini, S., Anglani, M., Cecchin, D., Corbetta, M., & Bertoldo, A. (2023). The dynamic functional connectivity fingerprint of high-grade gliomas. *Scientific Reports*, *13*(1), 10389.

Moretto, M., Silvestri, E., Zangrossi, A., Corbetta, M., & Bertoldo, A. (2022). Unveiling whole-brain dynamics in normal aging through Hidden Markov Models. *Human Brain Mapping*, *43*(3), 1129–1144.

Müller, F., Niso, G., Samiee, S., Ptito, M., Baillet, S., & Kupers, R. (2019). A thalamocortical pathway for fast rerouting of tactile information to occipital cortex in congenital blindness. *Nature Communications*, *10*(1), 5154.

Muret, D., & Makin, T. R. (2021). The homeostatic homunculus: rethinking deprivation-triggered reorganisation. *Current Opinion in Neurobiology*, *67*, 115–122.

Nakagawa, T. T., Jirsa, V. K., Spiegler, A., McIntosh, A. R., & Deco, G. (2013). Bottom up modeling of the connectome: linking structure and function in the resting brain and their changes in aging. *NeuroImage*, *80*, 318–329.

Neville, H., & Bavelier, D. (2002). Human brain plasticity: evidence from sensory deprivation and altered language experience. *Progress in Brain Research*, *138*, 177–188.

Noppeney, U. (2007). The effects of visual deprivation on functional and structural organization of the human brain. *Neuroscience and Biobehavioral Reviews*, *31*(8), 1169–1180.

Ortiz-Terán, L., Ortiz, T., Perez, D. L., Aragón, J. I., Diez, I., Pascual-Leone, A., & Sepulcre, J. (2016). Brain Plasticity in Blind Subjects Centralizes Beyond the Modal Cortices. *Frontiers in Systems Neuroscience*, *10*, 61.

Pant, R., Ossandón, J., Stange, L., Shareef, I., Kekunnaya, R., & Röder, B. (2023). Stimulus-evoked and resting-state alpha oscillations show a linked dependence on patterned visual experience for development. *NeuroImage. Clinical*, *38*, 103375.

Pelland, M., Orban, P., Dansereau, C., Lepore, F., Bellec, P., & Collignon, O. (2017). State-dependent modulation of functional connectivity in early blind individuals. *NeuroImage*, *147*, 532–541.

Quinn, A. J., Vidaurre, D., Abeysuriya, R., Becker, R., Nobre, A. C., & Woolrich, M. W. (2018). Task-Evoked Dynamic Network Analysis Through Hidden Markov Modeling. *Frontiers in Neuroscience*, *12*, 603.

Rączy, K., Hölig, C., Guerreiro, M. J. S., Lingareddy, S., Kekunnaya, R., & Röder, B. (2022). Typical resting-state activity of the brain requires visual input during an early sensitive period. *Brain Communications*, *4*(4), fcac146.

Radziun, D., Korczyk, M., Crucianelli, L., Szwed, M., & Ehrsson, H. H. (2023). Heartbeat counting accuracy is enhanced in blind individuals. *Journal of Experimental Psychology. General*, *152*(7), 2026–2039.

Raz, N., Amedi, A., & Zohary, E. (2005). V1 activation in congenitally blind humans is associated with episodic retrieval. *Cerebral Cortex (New York, N.Y.: 1991)*, *15*(9), 1459–1468.

Reich, L., Maidenbaum, S., & Amedi, A. (2012). The brain as a flexible task machine. *Current Opinion in Neurology*, *25*(1), 86–95.

Ricciardi, E., Handjaras, G., & Pietrini, P. (2014). The blind brain: how (lack of) vision shapes the morphological and functional architecture of the human brain. *Experimental Biology and Medicine (Maywood, N.J.)*, *239*(11), 1414–1420.

Rockland, K. S., & Ojima, H. (2003). Multisensory convergence in calcarine visual areas in macaque monkey. *International Journal of Psychophysiology: Official Journal of the International Organization of Psychophysiology*, *50*(1-2), 19–26.

Röder, B., Kekunnaya, R., & Guerreiro, M. J. S. (2021). Neural mechanisms of visual sensitive periods in humans. *Neuroscience and Biobehavioral Reviews*, *120*, 86–99.

Röder, B., Teder-Sälejärvi, W., Sterr, A., Rösler, F., Hillyard, S. A., & Neville, H. J. (1999). Improved auditory spatial tuning in blind humans. *Nature*, *400*(6740), 162–166.

Savva, A. D., Mitsis, G. D., & Matsopoulos, G. K. (2019). Assessment of dynamic functional connectivity in resting-state fMRI using the sliding window technique. *Brain and Behavior*, *9*(4), e01255.

Schaefer, A., Kong, R., Gordon, E. M., Laumann, T. O., Zuo, X.-N., Holmes, A. J., Eickhoff, S. B., & Yeo, B. T. T. (2018). Local-Global Parcellation of the Human Cerebral Cortex from Intrinsic Functional Connectivity MRI. *Cerebral Cortex* , *28*(9), 3095–3114.

Shinn, M. (2023). Phantom oscillations in principal component analysis. *Proceedings of the National Academy of Sciences of the United States of America*, *120*(48), e2311420120.

Smitha, K. A., Akhil Raja, K., Arun, K. M., Rajesh, P. G., Thomas, B., Kapilamoorthy, T. R., & Kesavadas, C. (2017). Resting state fMRI: A review on methods in resting state connectivity analysis and resting state networks. *The Neuroradiology Journal*, *30*(4), 305–317.

Striem-Amit, E., Ovadia-Caro, S., Caramazza, A., Margulies, D. S., Villringer, A., & Amedi, A. (2015). Functional connectivity of visual cortex in the blind follows retinotopic organization principles. *Brain: A Journal of Neurology*, *138*(Pt 6), 1679–1695.

Stroh, A.-L., Radziun, D., Korczyk, M., Crucianelli, L., Ehrsson, H. H., & Szwed, M. (2024). Blind individuals' enhanced ability to sense their own heartbeat is related to the thickness of their occipital cortex. *Cerebral Cortex (New York, N.Y.: 1991)*, *34*(8). https://doi.org/10.1093/cercor/bhae324

Taghia, J., Cai, W., Ryali, S., Kochalka, J., Nicholas, J., Chen, T., & Menon, V. (2018). Uncovering hidden brain state dynamics that regulate performance and decision-making during cognition. *Nature Communications*, *9*(1), 2505.

Tian, M., Xiao, X., Hu, H., Cusack, R., & Bedny, M. (2024). *Visual experience shapes functional connectivity between occipital and non-visual networks*. https://doi.org/10.7554/elife.93067.1

Van Schependom, J., Vidaurre, D., Costers, L., Sjøgård, M., D'hooghe, M. B., D'haeseleer, M., Wens, V., De Tiège, X., Goldman, S., Woolrich, M., & Nagels, G. (2019). Altered transient brain dynamics in multiple sclerosis: Treatment or pathology? *Human Brain Mapping*, *40*(16), 4789–4800.

Venkatesh, M., Jaja, J., & Pessoa, L. (2020). Comparing functional connectivity matrices: A geometry-aware approach applied to participant identification. *NeuroImage*, *207*, 116398.

Vidaurre, D. (2021). A new model for simultaneous dimensionality reduction and time-varying functional connectivity estimation. *PLoS Computational Biology*, *17*(4), e1008580.

Vidaurre, D., Llera, A., Smith, S. M., & Woolrich, M. W. (2021). Behavioural relevance of spontaneous, transient brain network interactions in fMRI. *NeuroImage*, *229*, 117713.

Vidaurre, D., Quinn, A. J., Baker, A. P., Dupret, D., Tejero-Cantero, A., & Woolrich, M. W. (2016). Spectrally resolved fast transient brain states in electrophysiological data. *NeuroImage*, *126*, 81–95.

Vidaurre, D., Smith, S. M., & Woolrich, M. W. (2017). Brain network dynamics are hierarchically organized in time. *Proceedings of the National Academy of Sciences of the United States of America*, *114*(48), 12827–12832.

Watanabe, T., & Rees, G. (2017). Brain network dynamics in high-functioning individuals with autism. *Nature Communications*, *8*, 16048.

Wen, Z., Zhou, F.-Q., Huang, X., Dan, H. D., Xie, B.-J., & Shen, Y. (2018). Altered functional connectivity of primary visual cortex in late blindness. *Neuropsychiatric Disease and Treatment*, *14*, 3317–3327.

Wittenberg, G. F., Werhahn, K. J., Wassermann, E. M., Herscovitch, P., & Cohen, L. G. (2004). Functional connectivity between somatosensory and visual cortex in early blind humans. *The European Journal of Neuroscience*, *20*(7), 1923–1927.

Xu, Y., Vignali, L., Sigismondi, F., Crepaldi, D., Bottini, R., & Collignon, O. (2023). Similar object shape representation encoded in the inferolateral occipitotemporal cortex of sighted and early blind people. *PLoS Biology*, *21*(7), e3001930.

Yeo, B. T. T., Krienen, F. M., Sepulcre, J., Sabuncu, M. R., Lashkari, D., Hollinshead, M., Roffman, J. L., Smoller, J. W., Zöllei, L., Polimeni, J. R., Fischl, B., Liu, H., & Buckner, R. L. (2011). The organization of the human cerebral cortex estimated by intrinsic functional connectivity. *Journal of Neurophysiology*, *106*(3), 1125–1165.

Zalesky, A., Fornito, A., & Bullmore, E. T. (2010). Network-based statistic: identifying differences in brain networks. *NeuroImage*, *53*(4), 1197–1207.

Zhang, Z., Zhang, D., Wang, Z., Li, J., Lin, Y., Chang, S., Huang, R., & Liu, M. (2018). Intrinsic neural linkage between primary visual area and default mode network in human brain: Evidence from visual mental imagery. *Neuroscience*, *379*, 13–21.